IMPLEMENTATION OF THE CDA PROCEDURE IN THE EMTP

Jiming Lin, Member, IEEE
Electric Power Research Institute
Beijing, China

José R. Martí, Member, IEEE
The University of British Columbia
Vancouver, B.C., Canada

Abstract - The CDA procedure eliminates the numerical oscillations that can occur in transients simulations that use the trapezoidal rule of integration. The CDA technique has been successfully implemented in the production code of the DCG/EPRI EMTP. This paper describes the details of this implementation for linear elements, nonlinear reactors, frequency dependent transmission lines, and synchronous machines. Simulation results involving these components are presented, showing the effectiveness of the procedure.

Keywords - Critical damping adjustment (CDA); numerical oscillations; EMTP simulations.

1 INTRODUCTION

Reference [1] presented the concept of "Critical Damping Adjustment" (CDA) to prevent numerical oscillations of the trapezoidal rule of integration at discontinuities. The CDA procedure allows the solution of the system of differential equations to proceed smoothly through discontinuities without introducing numerical damping in the solution. The advantages of this scheme over traditional techniques which introduce numerical damping in the solution were discussed in [1].

The present paper discusses the implementation of the CDA scheme for some of the major equipment models in the EMTP. These include nonlinear elements, frequency dependent transmission lines, and synchronous machines. Simulation results involving these elements are also presented.

Due to space limitations, details of the implementation of the CDA procedure for other elements in the EMTP, such as multiphase π-circuits, hysteresis loops, and the Universal Machine model, have been omitted. The required modifications for these elements are similar to the ones explained in the paper.

2 THE CRITICAL DAMPING ADJUSTMENT PROCEDURE (CDA)

To solve for the transient response of an electric circuit with the EMTP, the differential equations of each circuit component are first converted into difference equations. These difference equations involve simple algebraic relationships between voltages and currents at the time instant at which the system is solved. In a nodal formulation the network matrix equations at a given time instant t can be written as

$$[G][v(t)] = [i(t)] + [h(t)], \tag{1}$$

where [G] = constant matrix of equivalent node conductances; [v(t)] = vector of node voltages; [i(t)] = vector of external source currents; and [h(t)] = vector of history terms. The history terms h(t) are known from past values of branch voltages and currents. The value of the elements of [G] and [h(t)] depends on the numerical integration (or differentiation) rule used to discretize the differential equations.

Even though the trapezoidal rule of integration has excellent characteristics in terms of accuracy and stability, it does not respond well to discontinuities. These include switching operations, discontinuities in the values of the applied sources (including at $t = 0$), and transitions from one segment to another in piecewise linear inductances. In these cases, trapezoidal can oscillate to the overshoot produced by the discontinuity and maintain these oscillations with little or no damping. The CDA scheme solves these problems by completely dampening out the overshoot in two $\Delta t/2$ time steps. No traces of the overshoot are seen in the results after the second $\Delta t/2$ time step, and the simulation can proceed again with trapezoidal.

The application of the CDA procedure does not interfere with the normal solution scheme in the EMTP and does not require the resetting of initial conditions or other complications.

In the EMTP solution with the CDA scheme, the system is solved normally with the trapezoidal rule at time steps $t = 0$, Δt, $2\Delta t$, ..., etc. until a discontinuity is scheduled to occur at time t_1^+. The network is solved normally at t_1, assuming the discontinuity has not yet occurred (solution for t_1^-). Next, the discontinuity is applied and the CDA procedure is brought in to dampen out the overshoot.

With the network modified to take into account the new condition (for example, a switch change from open to closed), the next solution point is found at $t_1+\Delta t/2$ using the backward Euler rule.

The equivalent conductances of the network elements using the backward Euler rule with a step width of $\Delta t/2$ is identical to the equivalent conductances of these elements using the trapezoidal rule with a step width of Δt. Therefore, matrix [G] in eq. (1) does not change. Only the formula to evaluate the elements in the history vector [h(t)] needs to be changed.

The network is solved a second time with the backward Euler rule using a step size $\Delta t/2$, that is, at $t_2 = (t_1+\Delta t/2)+\Delta t/2$. Afterwards, the simulation continues normally with the trapezoidal rule at $t_2+\Delta t$, $t_2+2\Delta t$, $t_2+3\Delta t$, ..., etc., until another discontinuity is encountered.

The results at $t_1+\Delta t/2$ are only mathematical quantities used by the CDA procedure but have no physical meaning. Therefore, no decisions on whether to open or close switches, etc. are made based on these results. The next decisions are made at $t_1+\Delta t$, when the overshoot has already been dampened. An exception to this rule is the case of piecewise linear inductances, for which transitions from one segment to another at $t_1+\Delta t/2$ are allowed in order to avoid excessive deviations from the characteristic curve [3].

89 SM 667-7 PWRS A paper recommended and approved by the IEEE Power System Engineering Committee of the IEEE Power Engineering Society for presentation at the IEEE/PES 1989 Summer Meeting, Long Beach, California, July 9 - 14, 1989. Manuscript submitted January 31, 1989; made available for printing June 20, 1989.

3 LUMPED LINEAR ELEMENTS

The discretization of lumped linear elements with the trapezoidal and backward Euler rules was discussed in [1]. Figure 1 shows an inductance and its corresponding discrete-time model.

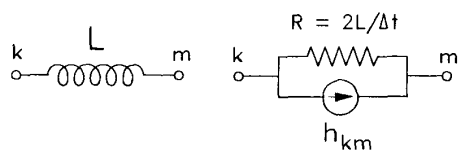

Fig. 1 Discrete-time equivalent circuit for an inductance.

The model in Fig. 1 results from applying the trapezoidal rule of integration for a step size Δt to the differential equation $v_{km}(t) = L\, di_{km}(t)/dt$. The discrete-time relationship is given by

$$i_{km}(t) = \frac{\Delta t}{2L} v_{km}(t) + h_{km}(t), \tag{2}$$

with a history term

$$h_{km}(t) = i_{km}(t-\Delta t) + \frac{\Delta t}{2L} v_{km}(t-\Delta t). \tag{3}$$

Equation (2) is inserted directly into the network nodal matrix (eq. (1)) to model the inductance branch.

Discretization of the differential equation of the inductance using the backward Euler rule for a step size $\Delta t/2$ gives exactly the same discrete-time relationship as in eq. (2). The only difference is in the history term, which is now given by

$$h'_{km}(t) = i_{km}(t-\Delta t/2). \tag{4}$$

The process of discretization of a continuous-time differential equation into a discrete-time difference equation using the trapezoidal rule for Δt and the backward Euler rule for $\Delta t/2$ is illustrated in the Appendix.

Comparing the history terms of trapezoidal (eq. (3)) and backward Euler (eq. (4)), it is seen that backward Euler uses only the history of the branch current, while trapezoidal includes the history of both the branch voltage and the branch current.

The equivalent resistance model of Fig. 1 is valid for both trapezoidal and backward Euler and therefore there is no change in the network's [G] matrix of eq. (1) due to the change of integration rule. The only change is in the history vector [h(t)].

The treatment of a capacitive branch is completely analogous to that of the inductance branch. The derivation of the corresponding relationships for general R-L-C branches is also straightforward. The procedure can also be easily extended to inductively coupled branches, which have the same relationships as the basic inductance but in matrix form.

4 NONLINEAR INDUCTANCES

A nonlinear inductance represented as straight-line segments [4] is shown in Fig. 2. The application of the CDA procedure to this element is discussed next.

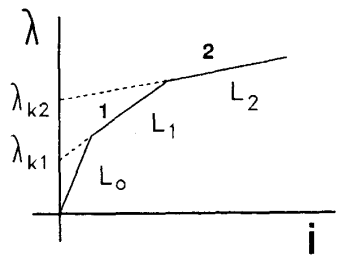

Fig. 2 Nonlinear inductance with piecewise linear characteristic.

In terms of flux linkages, the general equation for an inductance (linear or nonlinear) connected between nodes k and m is

$$v_{km}(t) = \frac{d\lambda(t)}{dt}, \tag{5}$$

where $\lambda = f(i)$.

Integrating eq. (5) with the trapezoidal rule for a full time step width Δt gives

$$\lambda(t) = \frac{\Delta t}{2} v_{km}(t) + h_\lambda(t), \tag{6}$$

where

$$h_\lambda(t) = \lambda(t-\Delta t) + \frac{\Delta t}{2} v_{km}(t-\Delta t). \tag{7}$$

Integrating eq. (5) with the backward Euler rule for $\Delta t/2$ gives the same result as in eq. (6), but with a history term given by

$$h'_\lambda(t) = \lambda(t-\Delta t/2). \tag{8}$$

The overall network solution (eq. (1)) is formulated in terms of voltages and currents. To obtain eq. (6) in terms of v and i, λ can be expressed in terms of its piecewise approximation. Assuming operation in segment 1 in Fig. 2,

$$\lambda(t) = \lambda_{k1} + L_1 i(t). \tag{9}$$

Replacing this relationship in eq. (6) gives

$$i(t) = \frac{\Delta t}{2L_1} v_{km}(t) + \frac{1}{L_1} h_\lambda(t) - \frac{\lambda_{k1}}{L_1}, \tag{10}$$

with $h_\lambda(t)$ given by eq. (7) for trapezoidal with Δt or by eq. (8) for backward Euler with $\Delta t/2$.

Equation (10) can be more simply expressed as

$$i(t) = \frac{\Delta t}{2L_1} v_{km}(t) + h(t), \tag{11}$$

with h(t) grouping the corresponding terms.

When during the normal solution with trapezoidal it is detected from the updated value of $\lambda(t)$ in eq. (9) that operation has to move from one segment to the other, for example from 1 to 2 in Fig. 2, the backward Euler rule is used for the solution in the next two $\Delta t/2$ steps with the new region parameters (L_2, λ_2).

If, after initiating the CDA procedure due to a change in operating region of the characteristic, a change to yet another region is detected after the first $\Delta t/2$ backward Euler step, three additional $\Delta t/2$ backward Euler steps are performed. The first two steps are sufficient to dampen the discontinuity created by the double switching of regions. The additional third step is performed in order to catch up with the evenly spaced (Δt) points of the normal trapezoidal solution.

TEST EXAMPLE:

Figure 3(a) shows a test system with a nonlinear reactor. Switches BL8B-BL8L close at t = 0.0194 s. Voltages at the reactor bus are shown in Figs. 3(b) and 3(c). Figure 3(b) shows the results obtained with the standard EMTP. Figure 3(c) shows the results obtained with the new EMTP using the CDA procedure. The numerical oscillations are completely eliminated without distorting the correct simulation results.

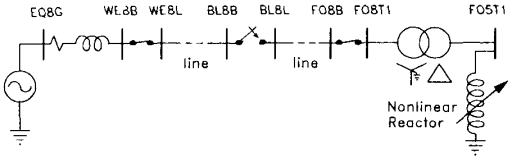

Fig. 3(a) Transient in system with nonlinear reactor.

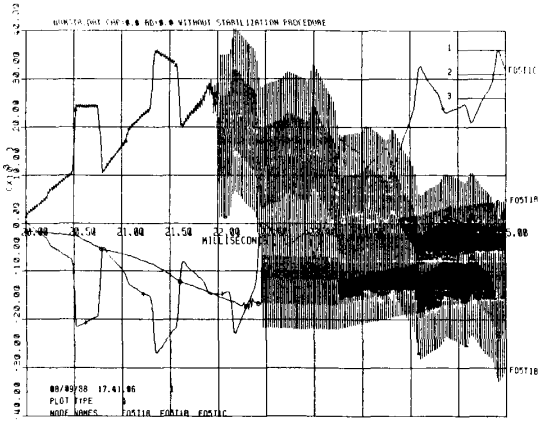

Fig. 3(b) Voltages at reactor bus. Standard EMTP.

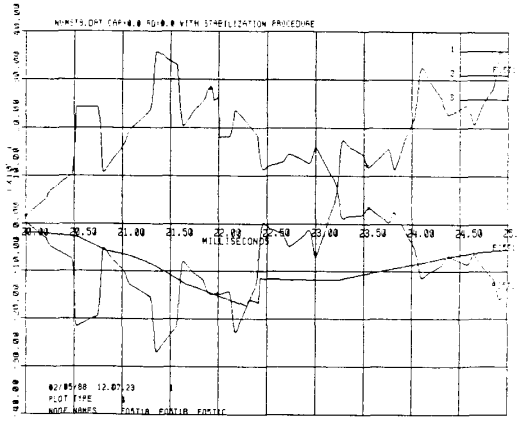

Fig. 3(c) Voltages at reactor bus. New EMTP with CDA.

5 FREQUENCY DEPENDENT TRANSMISSION LINES

A transmission line with distributed frequency dependent parameters R(ω), L(ω), G, C is shown in Fig. 4. It is assumed that the original multiphase line has been decoupled through diagonalizing matrix transformations and each mode can be analyzed separately.

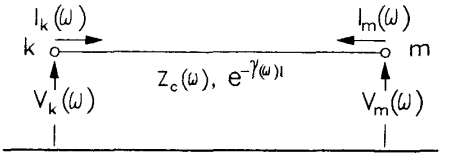

Fig. 4 Frequency dependent transmission line.

The application of the CDA procedure to the frequency dependent line model of [5] in the EMTP (fd-line model) is considered next. In the derivation of this model, voltages and currents at each line end are first related by

$$\begin{aligned} & V_m(\omega) + Z_c(\omega)(-I_m(\omega)) \\ & \quad = (V_k(\omega) + Z_c(\omega) I_k(\omega)) e^{-\gamma(\omega)\ell} \\ & \quad = F_k(\omega) e^{-\gamma(\omega)\ell} \\ & \quad = F_k(\omega) A(\omega) = E_{mk}(\omega) \end{aligned} \tag{12}$$

for node m, and similarly for node k. In this equation, $Z_c(\omega) = \sqrt{[R(\omega)+j\omega L(\omega)]/[G+j\omega C]}$ is the characteristic impedance, and $A(\omega) = e^{-\gamma(\omega)\ell}$, with $\gamma(\omega) = \sqrt{[R(\omega)+j\omega L(\omega)][G+j\omega C]}$, is the propagation function for a line length ℓ.

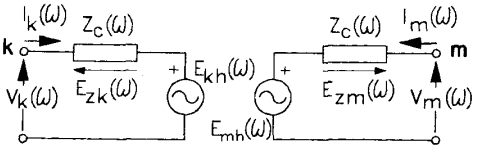

Fig. 5 Line equivalent circuit in the frequency domain.

Equation (12) for node m (and the corresponding equation for node k) give the line representation of Fig. 5.

Transferring the equivalent circuit of Fig. 5 to the time domain, and with $z_c(t) = \mathcal{F}^{-1}\{Z_c(\omega)\}$ and $a(t) = \mathcal{F}^{-1}\{e^{-\gamma(\omega)\ell}\}$, it is obtained for node m

$$v_m(t) = e_{zm}(t) + e_{mh}(t), \tag{13}$$

where

$$e_{zm}(t) = z_c(t) * i_m(t) \tag{14}$$

is the voltage drop in the equivalent impedance, and

$$e_{mh}(t) = f_k(t) * a(t) \tag{15}$$

is the equivalent history source. The symbol "*" in eqs. (14) and (15) above indicates time convolution. Similar relations are obtained for node k.

The function $f_k(t)$ in eq. (15) is formally defined in eq. (12) in the frequency domain. However, this function is more easily calculated directly from the voltage and current in the equivalent circuit at node k (Fig. 5):

$$F_k = V_k + Z_c I_k = V_k + (V_k - E_{kh}) = 2V_k - E_{kh},$$

or, transferring to the time domain,

$$f_k(t) = 2v_k(t) - e_{kh}(t). \tag{16}$$

The propagation function a(t) introduces a time delay (travelling time of the waves) on the function $f_k(t)$ (eq. (15)). As a result, the history source $e_{mh}(t)$ at time t is completely defined from past values of the quantities at node k.

Instead of performing the time domain convolutions indicated in eqs. (14) and (15), the frequency domain functions $Z_c(s)$ and A(s) ($s = j\omega$) are approximated by rational functions of s with simple negative poles and zeroes. These functions are then expanded into partial fractions. For the characteristic impedance,

$$Z_c(s) = k_0 + \sum_{j=1}^{n} \frac{k_j}{s + p_j}, \tag{17}$$

and for the propagation function,

$$A(s) = \left[\sum_{i=1}^{m} \frac{k_i}{s + p_i} \right] e^{-s\tau}, \tag{18}$$

where τ is the time delay of the line.

With $Z_c(s)$ expressed as in eq. (17), the s-plane form of eq. (14) is

$$E_{zm}(s) = k_0 I_m(s) + \sum_{j=1}^{n} E_{zmj}(s), \tag{19}$$

where each term $E_{zmj}(s)$ has the form

$$E_{zmj}(s) = \left[\frac{k_j}{s + p_j} \right] I_m(s). \tag{20}$$

These terms correspond to the first order differential equations

$$\frac{de_{zmj}(t)}{dt} + p_j e_{zmj}(t) = k_j i_m(t). \tag{21}$$

Equations (21) for each partial voltage term can now be discretized with an integration rule. Applying the trapezoidal rule with a full time step Δt gives

$$e_{zmj}(t) = \left[\frac{k_j}{2 + p_j \Delta t} \right] i_m(t) + h_{zmj}(t), \tag{22}$$

where the history term is

$$h_{zmj}(t) = \left[\frac{2 - p_j \Delta t}{2 + p_j \Delta t} \right] e_{zmj}(t - \Delta t) + \left[\frac{k_j \Delta t}{2 + p_j \Delta t} \right] i_m(t - \Delta t). \tag{23}$$

For the CDA procedure, eq. (21) is discretized with the backward Euler rule for $\Delta t/2$. This results in the same coefficient for $i_m(t)$ as in eq. (22). The only difference is in the history term, which is now given by

$$h'_{zmj}(t) = \left[\frac{2}{2 + p_j \Delta t} \right] e_{zmj}(t - \Delta t). \tag{24}$$

The partial voltage terms in eq. (22), together with k_0 in eq. (19), are added up to form the equivalent resistance in the final form of the line equivalent circuit in Fig. 6. This equivalent resistance is identical for trapezoidal with Δt and for backward Euler with $\Delta t/2$. Therefore, as in the case of lumped elements, the entries of the system [G] matrix in eq. (1) do not change during the CDA adjustment procedure.

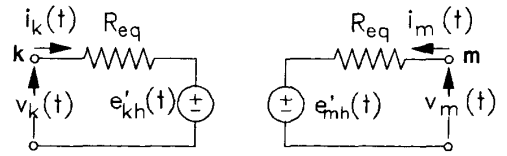

Fig. 6 Discrete-time equivalent for the fd-line model.

The above procedure to evaluate eq. (14) for $e_m(t)$ applies equally well to the evaluation of $e_{mh}(t)$ in eq. (15). In this latter case, A(s) in eq. (18) is applied to $F_k(s)$, and the resulting first order differential equations are then discretized using trapezoidal or backward Euler. Due to the time delay τ, all the terms in $e_{mh}(t)$ are history terms. The procedure can also be extended to include the frequency dependent transformation matrix model of [8].

The original implementation of the model of [5] in the EMTP used the "recursive convolution rule" to evaluate the convolutions in eqs. (14) and (15). This rule, however, is not compatible with the CDA procedure. If recursive convolution coefficients were used during the normal network solution, the equivalent resistance R_{eq} in Fig. 6 would not remain constant during the backward Euler stabilization steps. The use of the trapezoidal rule instead of the convolution rule in the present fd-line model, besides making the model compatible with the CDA procedure, results in better overall accuracy and resistance to machine truncation errors [7].

TEST EXAMPLE:

The circuit of Fig. 7(a) includes two frequency dependent line sections modelled with the JMARTI line model in the DCG/EPRI EMTP. Figures 7(b) and 7(c) show the voltages at nodes SIX-A,B,C. Switches THR-SIX open at t = 0.006 s. Figure 7(b) corresponds to the standard EMTP solution, and Fig. 7(c) corresponds to the solution with the new EMTP with the CDA procedure.

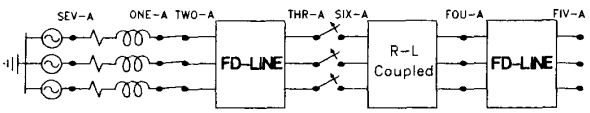

Fig. 7(a) Transients in system with frequency dependent lines.

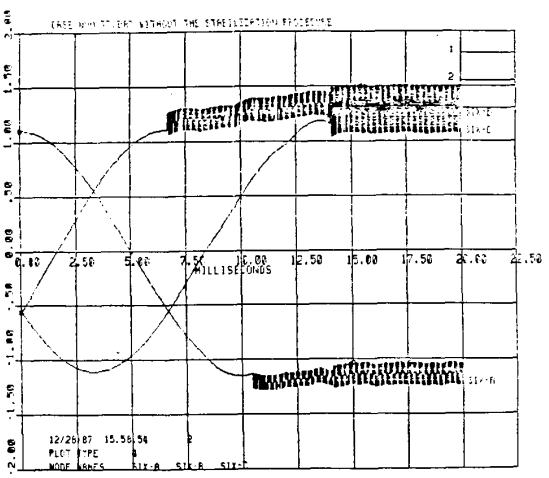

Fig. 7(b) Voltages in the line. Standard EMTP.

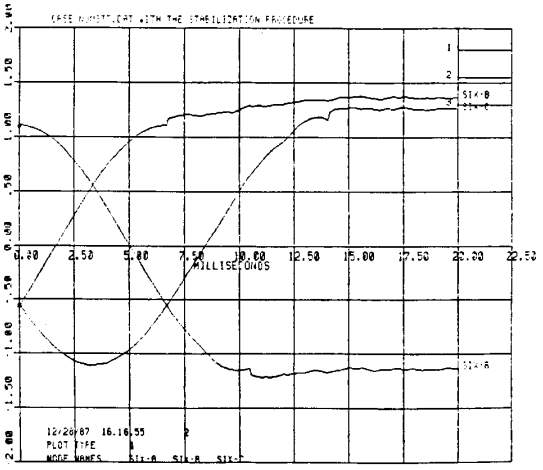

Fig. 7(c) Voltages in the line. New EMTP with CDA.

6 SYNCHRONOUS MACHINES

The three-phase synchronous machine model in the EMTP [9] involves two parts: (1) the electrical part, and (2) the mechanical part.

6.1 ELECTRICAL PART

The electrical part of the machine is modelled as seven coupled windings [6,9]. These windings are three armature windings (1,2,3), one field winding (f), two damper windings in the quadrature axis (g,Q), and one damper winding in the direct axis (D).

Transforming the equations of these seven machine windings to d,q,o variables gives

$$[v_{dqo}(t)] = -[R_{dqo}][i_{dqo}(t)] - \frac{d}{dt}[\lambda_{dqo}(t)] + \begin{bmatrix} -\omega\lambda_q(t) \\ +\omega\lambda_d(t) \\ 0 \\ 0 \\ 0 \\ 0 \\ 0 \end{bmatrix}, \quad (25)$$

with $[i_{dqo}] = [i_d, i_q, i_o, i_f, i_D, i_g, i_Q]$, and analogously for v and λ.

Consider first rows 1, 4, and 5 for the direct axis.

$$\begin{bmatrix} v_d(t) \\ v_f(t) \\ 0 \end{bmatrix} = -\begin{bmatrix} R_a & 0 & 0 \\ 0 & R_f & 0 \\ 0 & 0 & R_o \end{bmatrix}\begin{bmatrix} i_d(t) \\ i_f(t) \\ i_o(t) \end{bmatrix} - \begin{bmatrix} L_d & L_{df} & L_{do} \\ L_{df} & L_{ff} & L_{fo} \\ L_{do} & L_{fo} & L_{DD} \end{bmatrix}\frac{d}{dt}\begin{bmatrix} i_d(t) \\ i_f(t) \\ i_o(t) \end{bmatrix} + \begin{bmatrix} u_d(t) \\ 0 \\ 0 \end{bmatrix}. \quad (26)$$

with the speed voltage $u_d(t) = -\omega\lambda_q(t)$. In short-form notation,

$$[v(t)] = -[R][i(t)] - [L]\frac{d}{dt}[i(t)] + [u(t)]. \quad (27)$$

For the EMTP solution, the differential equations are first discretized. Discretization of eq. (27) with the trapezoidal rule for a step size Δt gives

$$[v(t)] = -\left([R] + \frac{2}{\Delta t}[L]\right)[i(t)] + [u(t)] + [h(t)], \quad (28)$$

with the history term given by

$$[h(t)] = \left(-[R] + \frac{2}{\Delta t}[L]\right)[i(t-\Delta t)] + [u(t-\Delta t)] - [v(t-\Delta t)]. \quad (29)$$

During the critical damping adjustment procedure, eq. (27) is discretized with the backward Euler rule using a step size of $\Delta t/2$. This gives the same form for eq. (28), except for the history term, which is now given by

$$[h'(t)] = \frac{2}{\Delta t}[L][i(t-\Delta t/2)]. \quad (30)$$

The derivation of the equations for the q-axis variables is analogous to the derivation for the d-axis variables, except that now both rotor voltages $v_g(t)$ and $v_Q(t)$ are zero, whereas in eq. (26) only $v_D(t)$ is zero.

For the zero sequence quantities, there is only one equation:

$$v_o(t) = -R_a i_o(t) - L_o\frac{di_o(t)}{dt}. \quad (31)$$

(The subscript of R in this equation is "a" and not "o". This latter subscript is introduced later.)

Discretizing eq. (31) with the trapezoidal rule for a step size Δt,

$$v_o(t) = -\left(R_a + \frac{2L_o}{\Delta t}\right)i_o(t) + h_o(t), \quad (32)$$

where

$$h_o(t) = \left(\frac{2L_o}{\Delta t} - R_a\right)i_o(t-\Delta t) - v_o(t-\Delta t). \quad (33)$$

Discretizing eq. (31) with the backward Euler rule for a step size $\Delta t/2$ gives the same relationship for eq. (32), but with a history term

$$h'_o(t) = \frac{2L_o}{\Delta t}i_o(t-\Delta t/2). \quad (34)$$

6.1.1 INTERFACING WITH THE EXTERNAL NETWORK

To interface eqs. (27) and (31) and the quadrature axis equation (analogous to eq. (27)) with the network connected to the machine, the following procedure is followed:

(a) Since the rotor voltages in eq. (26) are known ($v_f(t)$ = specified excitation voltage, and $v_D(t) = 0$), the two rotor currents can be eliminated. This reduces eq. (26) to a single equation:

$$v_d(t) = -R_d(t)i_d(t) + u_d(t) + h_d(t), \quad (35)$$

with $h_d(t)$ as the history term. The analogous reduction in the quadrature axis produces

$$v_q(t) = -R_q i_q(t) + u_q(t) + h_q(t), \quad (36)$$

Equation (32) is also of the same form:

$$v_o(t) = -R_o i_o(t) + h_o(t) \quad (37)$$

($R_o = R_a + 2L_o/\Delta t$).

(b) By using predicted values for the speed voltages $u_d(t)$ and $u_q(g)$ in eqs. (35) and (36), the machine becomes a simple voltage source behind R_d on the direct axis, R_q on the quadrature axis, and R_0 in the zero sequence variables. If these three independent Thevenin equivalent circuits were directly converted into the phase domain (with the d,q,o inverse transformation), the resulting phase-domain 3×3 resistance matrix would be time-dependent as well as asymmetrical. This would make the machine representation incompatible with the solution for the rest of the network.

To avoid these problems, approximations have to be made. The first approximation consists of using an average resistance $(R_d+R_q)/2$ on both d and q axes. To compensate for this, a "saliency term", $-[(R_d-R_q)/2]i_d(t)$, is added to $u_d(t)$, and $-[(R_q-R_d)/2]i_q(t)$ is added to $u_q(t)$. Predicted currents are used to evaluate these saliency terms.

These approximations will produce a simple machine model consisting of three known voltage sources behind a 3×3 equivalent resistance matrix.

(c) The complete electric network is solved together with the simple machine model of (b).

(d) From the solution of the electric network at time t, the electromagnetic torque in the machine at time t is calculated and then used to integrate the mechanical part from t-Δt to t.

Because the form of the equations remains the same, the solution procedure above is identical for the trapezoidal rule with a step width of Δt as it is for the backward Euler rule with a step width of Δt/2. Again, the only difference is in the formulas for the history terms. Also, the speed voltages and "saliency terms" must be predicted over half a time step Δt/2 for backward Euler instead of over a full step Δt for trapezoidal.

As indicated above, prediction of present value of speed voltages and saliency terms is used to simplify the machine model. In the version of the DCG/EPRI EMTP where the CDA procedure was implemented, the trapezoidal rule of integration is used for these predictions.

The application of the CDA procedure is unrelated to the prediction schemes. The only modification required in the program is to take into account the change in step width, from Δt during the normal trapezoidal solution to Δt/2 for the backward Euler CDA steps and then back to Δt to continue with the normal trapezoidal solution. During the two backward Euler steps of the CDA procedure, the trapezoidal rule is still used for the predictions, even though backward Euler is used in the discretization of the machine equations.

6.1.2 MECHANICAL PART

In the synchronous machine mechanical part, the response of the n shaft-connected rotation masses is described by the rotational form of Newton's Second Law:

$$[J]\frac{d}{dt}[\omega(t)]+[D][\omega(t)]+[K][\theta(t)] = [T_{net}(t)]+\omega_s[D_s], \tag{38}$$

with the speeds of the masses

$$[\omega(t)] = \frac{d}{dt}[\theta(t)], \tag{39}$$

and the net torque

$$[T_{net}(t)] = [T_{turbine}(t)]-[T_{gen/exc}(t)], \tag{40}$$

where $[J]$ = diagonal matrix of moments of inertia, $[\theta]$ = vector of angular positions of the masses, $[\omega]$ = vector of speeds, [D] = tridiagonal matrix of damping coefficients, [K] = tridiagonal matrix of stiffness coefficients, $[T_{turbine}]$ = vector of torques applied to the turbine stages, $[T_{gen/exc}]$ = vector of electromagnetic torques of generator and exciter, $[D_s]$ = vector of speed-deviation self-damping coefficient, and ω_s = synchronous velocity of the shaft-mass system.

Applying the trapezoidal rule to eqs. (38) and (39) gives

$$\left(\frac{2}{\Delta t}[J]+[D]+\frac{\Delta t}{2}[K]\right)[\omega(t)] = [T_{net}(t)]+2\omega_s[D_s]+[h(t)], \tag{41}$$

with the history term given by

$$[h(t)] = \left(\frac{2}{\Delta t}[J]-[D]-\frac{\Delta t}{2}[K]\right)[\omega(t-\Delta t)] - 2[K][\theta(t-\Delta t)]+[T_{net}(t-\Delta t)]. \tag{42}$$

Applying the backward Euler rule with step size Δt/2 to eqs. (38) and (39) gives the same result for eq. (41), with a history term

$$[h'(t)] = \frac{2}{\Delta t}[J][\omega(t-\Delta t/2)]-[K][\theta(t-\Delta t/2)]. \tag{43}$$

Again, the CDA procedure with backward Euler leads to the same discrete-time relationships as in the normal solution with trapezoidal, except for the new formulas for the history terms.

TEST EXAMPLES:

Figure 8(a) shows a test system for the synchronous machine model. Figures 8(b) and 8(c) show the voltages at the synchronous machine terminals, nodes G-A,B,C. The transient is created by first opening switches S1 at t = 0.002 s and then closing switches S2 at t = 0.04 s. The simulation in Fig. 8(b) was obtained with the standard EMTP and the simulation in Fig. 8(c) was obtained with the new EMTP with the CDA procedure.

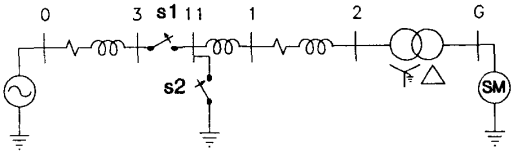

Fig. 8(a) Transients in system with synchronous machine.

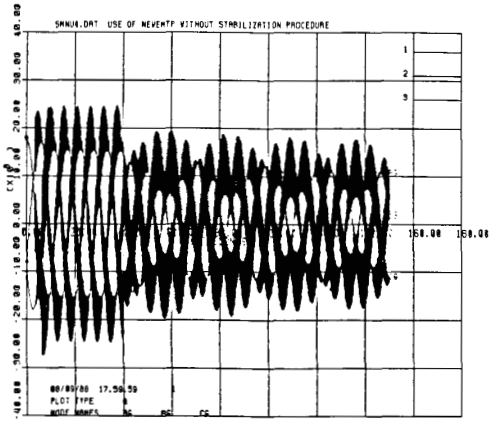

Fig. 8(b) Voltages at synchronous machine bus. Standard EMTP.

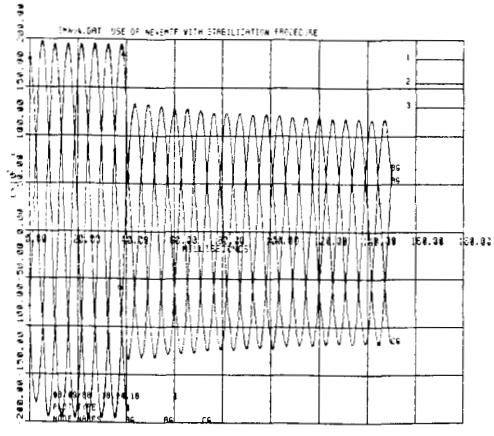

Fig. 8(c) Voltages at synchronous machine bus. New EMTP with CDA.

The principles of the Universal Machine model in the EMTP are described in references [6,10]. Even though the implementation of the CDA procedure for the Universal Machine model in the EMTP was not discussed in the paper, a test simulation has been included. Figure 9(a) shows the test circuit with an induction motor modelled with the Universal Machine model. In the simulation, switches BUS2-BUS3 open after t = 0.001 s. The results, for voltages at BUS2-A,B,C, are shown in Figs. 9(b) and 9(c). The results shown correspond to the prediction-based interface of the Universal Machine model. The simulation was also run using the compensation method interface with practically identical results.

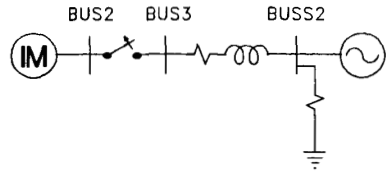

Fig. 9(a) Transients in system with induction motor (Universal Machine model).

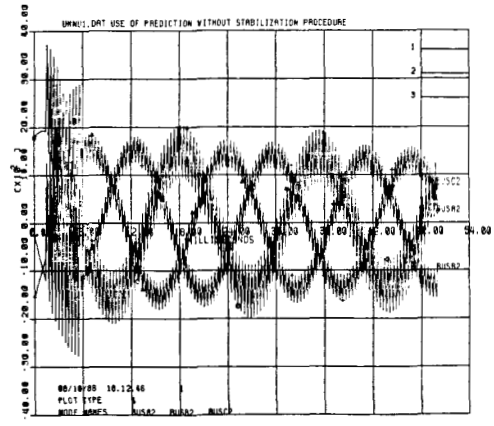

Fig. 9(b) Voltages at motor bus. Standard EMTP.

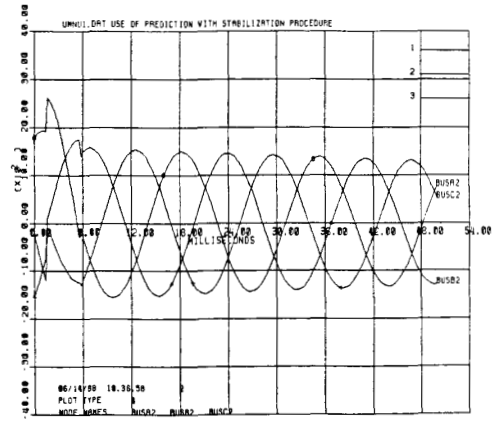

Fig. 9(c) Voltages at motor bus. New EMTP with CDA.

7 CONCLUSIONS

This paper has presented the application of the critical damping adjustment technique CDA to some of the main equipment models in the EMTP. The implementation was described for linear elements, nonlinear reactors, frequency dependent transmission lines, and for synchronous machines. As shown in the paper, even though some of the models are quite elaborate, the implementation of the CDA technique is straightforward.

The form of the discretized equations and the corresponding equivalent circuits are the same for trapezoidal with a step size of Δt and for backward Euler with a step size of $\Delta t/2$. The values of the conductances in the equivalent circuits are also the same in both cases. Only the history terms need to be changed.

Simulation results are presented showing the effectiveness of the CDA procedure in eliminating numerical oscillations in simulations involving nonlinear reactances, frequency dependent transmission lines, and synchronous machines.

APPENDIX

The relationship between the difference equations obtained with the trapezoidal rule of integration with a time step Δt and with the backward Euler rule of integration with a time step $\Delta t/2$ is illustrated next for the case of a series RL branch. The derivation for other models is analogous.

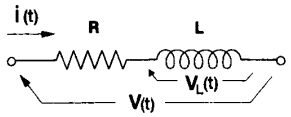

Fig. A.1 Series RL branch.

The voltage across the inductance L in Fig. A.1 is given by $v_L = L\, di/dt$. It then follows that $v_L\, dt = L\, di$ and

$$\int_{t-\Delta t}^{t} v_L\, du = L[i(t) - i(t-\Delta t)]. \tag{A.1}$$

The trapezoidal rule approximation to the integral in eq. (A.1) is

$$\int_{t-\Delta t}^{t} v_L\, du \simeq \frac{v_L(t) + v_L(t-\Delta t)}{2} \cdot \Delta t, \tag{A.2}$$

while the backward Euler approximation is

$$\int_{t-\Delta t}^{t} v_L\, du \simeq v_L(t) \cdot \Delta t. \tag{A.3}$$

For the trapezoidal rule, replacing eq. (A.2) in eq. (A.1) and relating the branch voltage to the branch current, the following discrete-time relationship is obtained for the RL branch of Fig. A.1

$$v(t) = \left(R + \frac{2L}{\Delta t}\right) i(t) + \left[-v(t-\Delta t) + \left(R - \frac{2L}{\Delta t}\right) i(t-\Delta t) \right], \tag{A.4}$$

where the terms in brackets are the history terms.

For the backward Euler rule, replacing eq. (A.3) in eq. (A.1), the discrete-time relationship for the RL branch is

$$v(t) = \left(R + \frac{L}{\Delta t}\right) i(t) + \left[-\left(\frac{L}{\Delta t}\right) i(t-\Delta t) \right]. \tag{A.5}$$

If in eq. (A.5) Δt is replaced by $\Delta t/2$, the result is

$$v(t) = \left(R + \frac{2L}{\Delta t}\right) i(t) + \left[-\left(\frac{2L}{\Delta t}\right) i(t-\Delta t) \right]. \tag{A.6}$$

Comparing eqs. (A.4) and (A.6), it is seen that, except for the history terms, they are identical.

ACKNOWLEDGEMENT

The implementation of the CDA technique described in the paper was done for the DCG/EPRI version of the EMTP. The authors are grateful to DCG/EPRI and to the Canadian Electrical Association CEA for their financial support in this project and for granting permission to publish this material. Our thanks also to Dr. Hermann Dommel for his guidance during the development of the project.

REFERENCES

[1] J.R. Martí, J. Lin, "Suppression of numerical oscillations in the EMTP," 88 SM 732-0 IEEE/PES 1988 Summer Meeting, July 1988.

[2] H.W. Dommel, "Digital computer solution of electromagnetic transients in single- and multi-phase networks", IEEE Trans., Vol. PAS- 88, pp. 388-399, April 1969.

[3] H.W. Dommel, *Digital Simulation of Electrical Transient Phenomena, chapter III: Extensions of the Basic Solution Methods,* (IEEE Pub. 81EH0173-5-PWR, 1980), pp. 20-29.

[4] H.W. Dommel, "Nonlinear and time-varying element in digital simulation of electromagnetic transients," IEEE Trans., Vol. PAS-90, pp. 2561-2567, Nov/Dec 1971.

[5] J.R. Martí, "Accurate modelling of frequency-dependent transmission lines in electromagnetic transient simulations", IEEE Trans., Vol. PAS-101, pp. 147-155, January 1982.

[6] H.W. Dommel, *Electromagnetic Transients Program Reference Manual (EMTP Theory Book),* (Bonneville Power Administration, Portland, Oregon, 1986).

[7] J.R. Martí, "Numerical integration rule and frequency-dependent line models," EMTP Newsletter, Vol. 5, No. 3, pp. 27-29, July 1985.

[8] L. Martí, "Simulation of transients in underground cables with frequency-dependent modal transformation matrices," IEEE Trans., Vol. 3, pp. 1099-1110, July 1988.

[9] V. Brandwajn, *Synchronous generator models for the analysis of electromagnetic transients,* (Ph.D. Thesis), (The University of British Columbia, Vancouver, B.C. Canada, 1977).

[10] H.K. Lauw, "Interfacing for universal multi-machine system modeling in an electromagnetic transient program," IEEE Trans., Vol. PAS-104, pp. 2367-2373, Sept. 1985.

Jiming Lin (M'88) was born in Fujian, China in 1941. He graduated in Electrical Engineering from Tsinghua University, Beijing, China in 1964.

In 1964 he joined the Electric Power Research Institute, Beijing, China. From 1964-82 he worked in the High Voltage Division in switching surges, and from 1982-86 in the Power Systems Division in power system analysis. From 1986 to 1988 he was at the University of British Columbia as a Visiting Scholar. At present he is with the Electric Power Research Institute, Beijing, China.

José R. Martí (M'71) was born in Spain in 1948. He received a M.E. degree from Rensselaer Polytechnic Institute in 1974 and a Ph.D. degree in Electrical Engineering from the University of British Columbia in 1981.

He worked for Industry from 1970 to 1972. In 1974-77 and 1981-84 he taught power system analysis at Central University of Venezuela. Since 1984 he has been with the University of British Columbia.

Discussion

Adam Semlyen (University of Toronto): I would like to commend the authors for having implemented their new approach, the Critical Damping Adjustment [1], in those parts of the EMTP where discontinuities may produce numerical oscillations. The application of the CDA to transmission lines is particularly interesting because it required abandoning the former approach of recursive convolutions in favor of a state equation formulation which is necessary for using both the trapezoidal rule and the backward Euler integration methods of the CDA.

By the use of state equations in the time domain as an equivalent of transfer functions in the frequency domain, transmission line modeling has made a full swing. Indeed, the basic frequency domain relations, in terms of a transfer function H, are of the form

$$Y = HU \tag{1}$$

and their time domain equivalent is of the form

$$y = hu + y_{hist} \tag{2}$$

which results from the discretization of the state equations

$$\dot{x} = Ax + Bu \tag{3a}$$

$$y = Cx + Du \tag{3b}$$

Equation (2) is of extreme simplicity and often translates to a Thevenin or Norton equivalent. The set {A,B,C,D} can be obtained by direct frequency domain fitting[A-D,5] of H.

The simplicity of the time domain equivalent (2) is surpassed only by the symbolic form used for convolutions:

$$y = h * u \tag{4}$$

This form can not be used directly for computations but it is convenient for derivations, as used also in the present paper. Based on such derivations, in earlier work of EMTP development full convolutions[E,F,G] and recursive convolutions[H,5] have been used. Full convolutions are computationally expensive but may be needed when a state equation approximation (or, equivalently, a rational fitting) of a given transfer function can not be obtained. Recursive convolutions are of course computationally more efficient but in general not better[D] than the state equations which are their equivalent[H].

The use of state equations does not imply restrictions to real poles even if only real arithmetic is used in the computations. The sum of a pair k of complex conjugate or real simple fractions, as in eqn.(17) of the paper, has the form

$$\frac{c''_k s + c'_k}{s^2 + \beta_k s + \gamma_k} \tag{5}$$

and can be obtained directly from the following state equations

$$\begin{bmatrix} \dot{x}_{1,k} \\ \dot{x}_{2,k} \end{bmatrix} = \begin{bmatrix} 0 & 1 \\ -\gamma_k & -\beta_k \end{bmatrix} \begin{bmatrix} x_{1,k} \\ x_{2,k} \end{bmatrix} + \begin{bmatrix} 0 \\ 1 \end{bmatrix} u \tag{6a}$$

$$y_k = [c'_k \;\; c''_k] \begin{bmatrix} x_{1,k} \\ x_{2,k} \end{bmatrix} \tag{6b}$$

by replacing the derivative by s. The resultant state equations of form (3), for all pairs k of simple fractions (5), is obtained by concatenating the corresponding matrices of equations (6): {A,B,C} = {diag(A_k), col(B_k),row(C_k)}.

The advantage of not restricting poles to the real axis[C,D] is that the same accuracy may be achieved with a lower order fitting. This may be crucial in real-time applications of transmission line modeling[I,J].

The authors' comments on the above remarks would be most appreciated.

[A] A. Semlyen, "Switching Surge Calculation with Exponential Response Functions Obtained by Direct Frequency Domain Fitting", Proceedings of the Canadian Communications and Power Conference, Montreal, November 1974, pp. 179-180.

[B] A. Morched and A. Semlyen, "Transmission Line Step Response Calculation by Least Square Frequency Domain Fitting", 1976 IEEE/PES Summer Meeting, Portland, Oregon, Paper No. A76 394-7.

[C] A. Semlyen and A. Roth, "Calculation of Exponential Propagation Step Responses - Accurately for Three Base Frequencies", IEEE Trans. on Power Apparatus and Systems, Vol. PAS-96, No. 2, March/April 1977, pp. 667-672.

[D] A. Semlyen, "Contributions to the Theory of Calculation of Electromagnetic Transients on Transmission Lines with Frequency Dependent Parameters", IEEE Trans. on Power Apparatus and Systems, Vol. PAS-100, No. 2, February 1981, pp. 848-856.

[E] A. Semlyen, "Accurate Calculation of Switching Transients in Power Systems", 1971 IEEE Winter Power Meeting, New York, Paper No. 71CP 87-PWR.

[F] W.S. Meyer and H.W. Dommel, "Numerical Modelling of Frequency-Dependent Transmission-Line Parameters in an Electromagnetic Transients Program", IEEE Trans. on Power Apparatus and Systems, Vol. PAS-99, No. 5, Sept./Oct. 1974, pp. 1401-1409.

[G] J.K. Snelson, "Propagation of Travelling Waves on Transmission Lines - Frequency Dependent Parameters", IEEE Trans. on Power Apparatus and Systems, Vol. PAS-91, No. 1, Jan/Feb. 1972, pp. 85-91.

[H] A. Semlyen and A. Dabuleanu, "Fast and Accurate Switching Transient Calculations on Transmission Lines with Ground Return Using Recursive Convolutions", IEEE Trans. on Power Apparatus and Systems, Vol. PAS-94, No. 2, March/April 1975, pp. 561-571.

[I] R.M. Mathur, Xuegong Wang, "Real-Time Digital Simulator of the Electromagnetic Transients of Power Transmission Lines", IEEE/PES 1988 Summer Meeting, Portland, Oregon, Paper No. 88 SM 584-5.

[J] Xuegong Wang, R.M. Mathur, "Real-Time Digital Simulator of the Electromagnetic Transients of Transmission Lines with Frequency Dependence", IEEE/PES 1989 Winter Meeting, New York, N.Y., Paper No. 89 WM 122-3 PWRD.

Manuscript received August 2, 1989.

J. Lin and J.R. Martí: Our thanks to Professor Semlyen for his interesting comments. Indeed, the modelling of frequency dependent transmission lines is making a full swing as the nature of frequency dependence modelling is better understood. In its present form in the DCG/EPRI EMTP, the line model of [5] has been reduced to a form that is equivalent to having a set of n linear first-order differential equations, as in the state-variable formulation of eqs. (3a) and (3b) in the Discussion. In effect, a first-order differential equation with parameters that are functions of frequency is being replaced by a set of n first-order differential equations with constant parameters. As indicated by Professor Semlyen, the link that allows this conversion is frequency-domain fitting by rational functions that can be expanded into simple first-order partial fractions. These partial fractions can correspond to either simple real poles or to pairs of complex conjugate poles.

In the work of reference [5] only simple real poles were used, mainly because of simplicity in designing the fitting algorithm. This algorithm does not need a guess of initial values of the parameters and can be easily controlled to assure convergence to a solution. Due to the smooth form of the line functions to be fitted, this simple algorithm provides very accurate results.

As Professor Semlyen points out, complex conjugate poles are equally valid alternatives to generate state equations and allow a greater degree of flexibility in the shaping of the fitting function $H(\omega)$. The availability of an extra parameter, the damping factor ζ, in addition to the corner frequency of the undampened pole, allows for a larger control of the shape of the fitting curve than what is possible with two real poles. This technique has been effectively explored by Professor Semlyen in the references mentioned in his Discussion.

The use of complex conjugate poles is particularly important when fitting transfer functions that present sharp peaks and valleys in their frequency response, such as those encountered in high-frequency transformer modelling or in network equivalents. The extension of the fitting routines of [5] to incorporate complex poles and zeroes in the fitting algorithm is currently under investigation.

Manuscript received August 31, 1989.